Mode-Locking in an Erbium-Doped Fiber Laser

Ethan Lane

Rose-Hulman Institute of Technology

Table Of Contents

I. Abstract

The Research and Development division requires a mode locked laser with pulse lengths on the order of 100 fs to sync with RF cavity pulses. The 1550 nm MENLO laser system originally meant for the work has obtained pulse lengths on the order of ~10 μs, orders of magnitude longer than desired. This project was designed with the goal in mind of fabricating the division's own 1550 nm mode-locked laser utilizing erbium-doped fiber as a gain medium in a fiber laser cavity. Erbium is a key choice due to the reduced cost of fiber from the telecommunications industry as well as the fact that it emits light at the desired wavelength of 1550 nm. This laser was fabricated in a stepwise fashion by installing, testing and modifying key parts until they met desired specifications. At optimal settings, pulse widths of less than 400 fs can be achieved, and future plans for the system focus on further modification of the laser setup so that smaller pulse widths can be achieved.

II. Introduction

In the Research and Development division of Fermilab, strides are constantly being taken to improve our current technology. One particular stride of interest, and the subject of this paper, is the construction of a mode-locked erbium-doped fiber laser. The main goal behind the construction of this laser is to achieve power pulses on the order of femtoseconds. The laser was constructed in a stepwise fashion broken into a series of tests.

In order to understand how the tests were performed and ideas behind them, a basic understanding of lasers, optical fibers, power, mode-locking, etc. must be obtained. This introduction includes the setup of the final product of this particular laser as well as how they relate to the basic parts of a laser. Theory behind wave propagation and mode-locking is also provided.

1. Parts to a Laser

Every laser has three basic parts, a lasing medium, a pump, and an optical cavity. The fiber laser fabricated in this experiment is no different. The 980 nm butterfly-mounted diode laser acts as a pump to the erbium laser. The lasing medium is the erbium fiber itself. The optical cavity in this case takes advantage of the properties of optical fiber and loops the beam through an amplifier back onto itself, whereas a free-space laser would likely use mirrors to make an optical cavity. Figure 1 depicts a simplified version of the schematic in the mode locking section, and illustrates how the laser parts are integrated together:

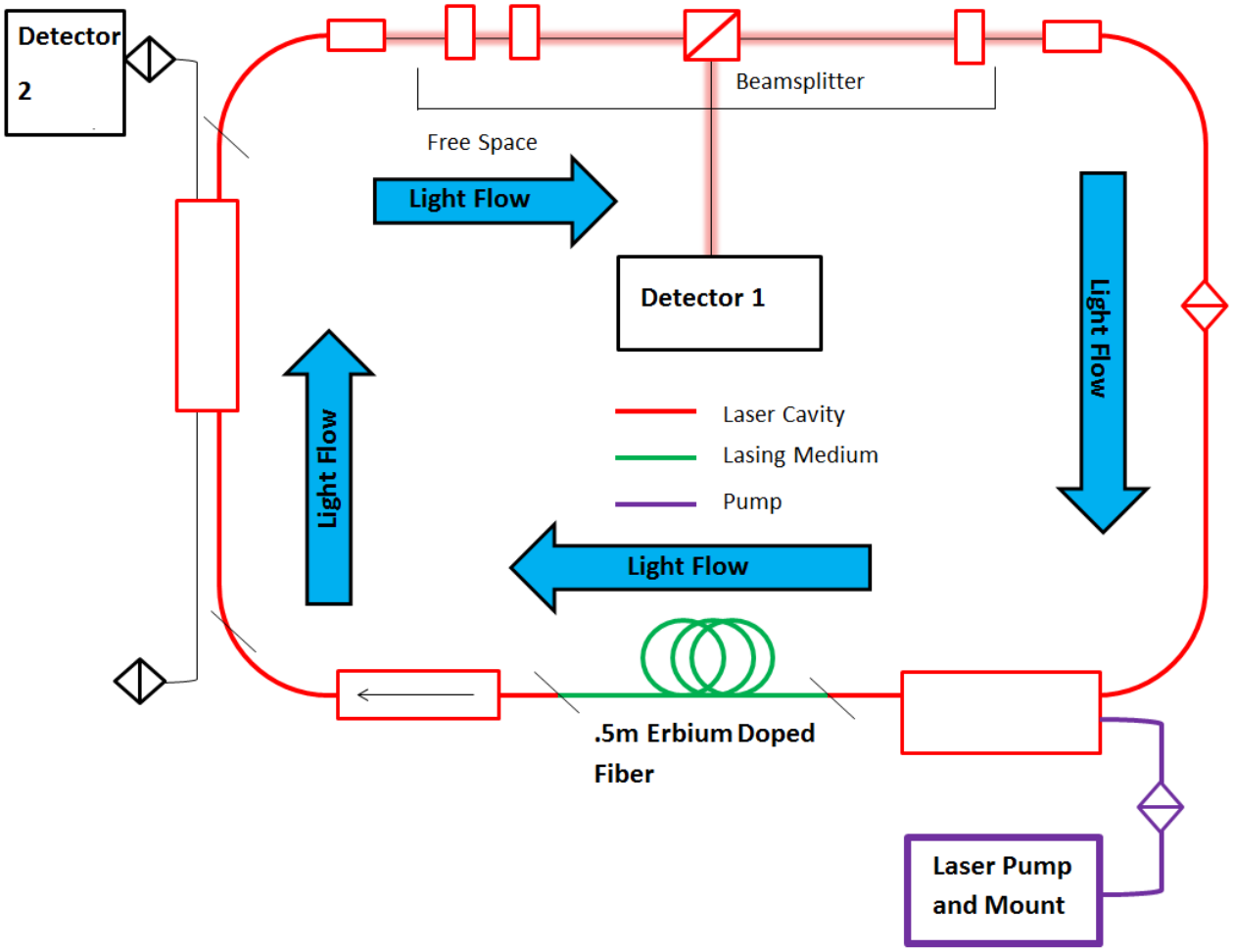

Figure 1. This is a simplified diagram of the mode-locked laser and shows the relationship of the laser parts.

2. System Setup

The final arrangement of parts used in this system began with a butterfly-mounted diode laser as the pump for the erbium laser. This was connected to a 980 nm patch cable[1] through an FC/APC connection[2]. The patch cable was spliced* to one input of a wavelength-division multiplexor (WDM)[3]. The output from the WDM was spliced to .5 meters of erbium-doped fiber which, in turn, was spliced to an isolator[4]. The output of the isolator was sliced to an output coupler[5] input lead. This output coupler released 90% of the incoming power through one lead and 10% through the other. The 10% output was connected through FC/APC to either an optical power meter or power spectrum analyzer, depending on the experiment. The 90% output lead was spliced to a collimator[6] which brought the beam into free space. In the free space section of the cavity, a quarter-wave plate[7], half-wave plate[8], beamsplitting cube[9], and another

quarter-wave plate were set up, respectively. The light from free space travelled into another collimator after going through this system. The collimator was then connected through an FC/APC connection back into the WDM to form the laser cavity. (see Figure 14 for more details)

1) The only type of patch cable used in this system. Certain patch cables are designed to only operate within a certain range of wavelengths. The 980 nm that was used in this system was able to operate at 980 nm as well as 1550 nm.
2) A standard type of connector for fiber optical media; analogous to an electrical wire connector.
3) Functions to take multiple fiber-optical input signals and output them into one signal.
4) Only allows an optical signal to travel in one direction through it; installed to prevent extra modes from being supported in different directions, as the cavity has a set amount of power that it can hold.
5) Couples light from two input leads into two outputs, one 90% of the power and the other 10% .
6) Focuses the light from a fiber input into a beam for free space lasing.
7) A phase retarder that elliptically polarizes light depending on the orientation.
8) A phase retarder that changes light polarization direction depending on its orientation
9) A cube that splits an incident beam into two parts; installed to output 10% of the incident beam into a photodiode connected to an oscilloscope.

* For information on splicing, see the Appendix B.

III. Theory

1. Wave Propagation

There are a great many factors that come into play when dealing with fiber lasers with short pulse lengths. Generally speaking, light propagation follows the Schrodinger wave equation:

$$\boldsymbol{\nabla}^2\boldsymbol{E} - \frac{1}{c^2}\frac{\partial^2}{\partial t^2}\boldsymbol{E} = \mu_0\frac{\partial^2}{\partial t^2}\boldsymbol{P}$$

where **E** is the electric field vector, **P** is the polarization vector, μ_0 the permeability of free space, and c is the speed of light. However, since we are dealing with such small pulses, nonlinear effects have to be taken into account. The nonlinear polarization is given by:

$$\boldsymbol{P}(\boldsymbol{r},t) = \epsilon_0\left(\chi^{(1)}\boldsymbol{E}(\boldsymbol{r},t)\right) + \chi^{(2)}\boldsymbol{E^2}(\boldsymbol{r},t) + \chi^{(3)}\boldsymbol{E^3}(\boldsymbol{r},t) + \cdots = \boldsymbol{P}_L + \boldsymbol{P}_{NL}$$

where the first-order term is equal to the linear polarization and the rest accounting for the nonlinear polarization. The second-order term, $\chi^{(2)}$, will be ignored as it deals with phase-matching, making it negligible for our purposes [1]. Now to make a few assumptions:

1) The response of the polarization is instant. There is no sort of memory effect or delay in response time. This works for ~ps pulses.
2) The nonlinear effects of **P** are small enough such that they can be treated as perturbations.
3) The field maintains its polarization along the entire fiber, so a scalar approach may be used.

With these assumptions in mind, the real part of the electric field can be broken into a slowly varying wave envelope, F(x,y), and a plane wave propagating in the z-direction, A(z,t):

$$\boldsymbol{E}(\boldsymbol{r},t) = \frac{1}{2}\boldsymbol{u}_x\left(E(\boldsymbol{r},t)e^{i(\beta_0 z-\omega_0 t)}\right) = \frac{1}{2}\boldsymbol{u}_x\left(F(x,y)A(z,t)e^{i(\beta_0 z-\omega_0 t)}\right)$$

where $\boldsymbol{u}_x$ is an arbitrary unit vector perpendicular to the direction of propagation, $\beta_0 = \frac{n\omega_0}{c}$ for index of refraction n, and ω_0 is the radial frequency of the propagating wave. This, after several applications of the Fourier transform, a Taylor series expansion, and use of the initial assumptions gives the nonlinear Schrodinger equation for picosecond pulses [1]:

$$\frac{\partial A}{\partial z} + \frac{i\beta_2}{2}\frac{\partial^2 A}{\partial T^2} + \frac{\alpha}{2}A = i\gamma|A|^2A$$

where $T = t - \frac{z}{v_g}$ for the group velocity of the wave, v_g, α is a fiber loss factor, $\beta_2$accounts for chromatic dispersion, and γ deals with fiber nonlinearities. The function F(x,y) closely follows a Gaussian curve, and is approximated as such.

The previously given Schrodinger wave equation does not take into account the time it takes for an electron cloud to reconfigure after being affected by a pulse, which is ~.1 fs. For short fs pulses, this is no longer negligible, and is referred to as the Raman Effect [1]. This has to do with third-order effects of the polarization, $\chi^{(3)}$. This effect changes the nonlinear Schrodinger equation to [1]:

$$\frac{\partial A}{\partial z} + \frac{i\beta_2}{2}\frac{\partial^2 A}{\partial T^2} + \frac{\alpha}{2}A - \frac{\beta_3}{6}\frac{\partial^3 A}{\partial T^3} = i\gamma(|A|^2 A + \frac{i}{\omega_0}\frac{\partial}{\partial T}(|A|^2 A) - T_R A\frac{\partial |A|^2}{\partial T})$$

where β_3 is the third-order dispersion term, and T_R is defined to be the first momentum of the nonlinear response function. Upon inspection, one can see that this simply adds in a few extra terms into the previous nonlinear Schrodinger equation. The net effect of these terms is to cause a slight asymmetry in the Gaussian curve for the slowly varying wave envelope called self steepening, where the peak shifts slightly [1].

The last effect that must be taken into account for mode-locked pulses is the effect that gain has on the nonlinear Schrodinger equation. Now a third term is added to the induced polarization,

$$\mathbf{P_d}(\mathbf{r},t) = \frac{1}{2}\boldsymbol{u}_x\left(\boldsymbol{P}_d(\boldsymbol{r},t)e^{i(\beta_0 z - \omega_0 t)}\right)$$

which takes into account the effects of the dopants in the fiber length. The effect that this has is to yield new effective β coefficients, the equations for which are very complicated and vary with the fiber length [1]. These coefficients describe the dispersive effect that doping has on a pulse propagating through a fiber. The case of positive dispersion will cause the pulse to widen, yielding longer pulse lengths. Similarly, negative dispersion will give shorter pulse lengths.

2. Mode-Locking

The only way in which to achieve picosecond or smaller pulse lengths in a laser is to perform what is called mode-locking, or the act of locking all wavelengths in a laser cavity to a fixed phase relation. In a normal laser (i.e. not mode-locked), light is emitted in the lasing medium with random phase differences between the electric fields for each individual photon. Mode-locking is a method by which the phases obtain a fixed relation, so the electric field experiences large spikes in amplitude followed by a period of little to no amplitude instead of the fairly uniform amplitude it experiences otherwise. Figure 2 depicts this effect.

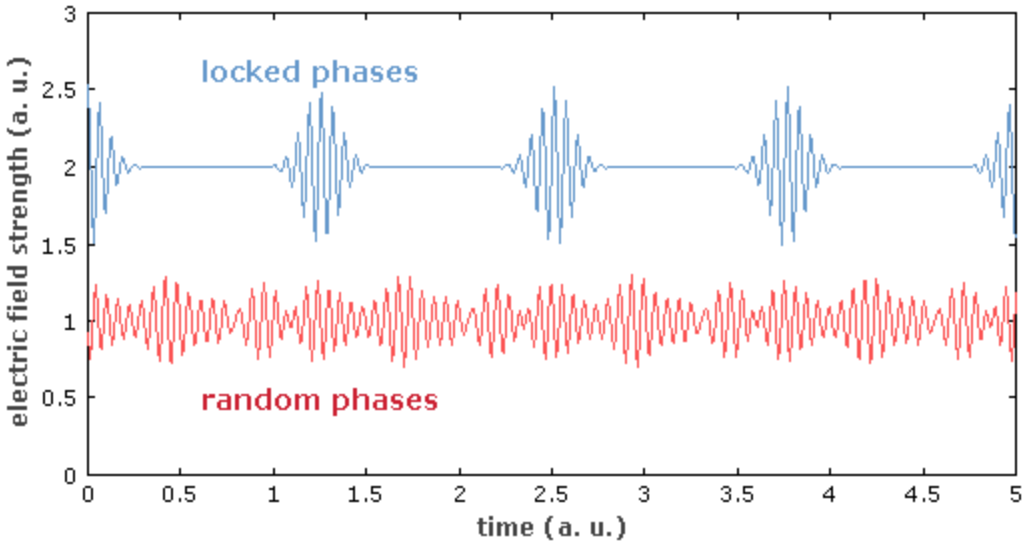

Figure 2. This shows the differences in electric field strength in time with random phase relations versus a fixed phase.

By virtue of the wave nature of light, the total electric field in this situation can be described by the summation of all 2n+1 (for mathematical simplicity) modes of a cavity with phase ϕ_m, propagation constant k_m, and radial frequency ω_m, or:

$$E(t) = \sum_{-n}^{n} E_m e^{i(k_m z - \omega_m t + \varphi_m)}$$

Using the assumption that the amplitudes are equal for all modes, simplifying using a geometric series, and Euler's formula, the magnitude of the total electric field becomes:

$$|E(t)| = E_0 \frac{\sin[(2n+1)\pi f_{rep} t']}{\sin[\pi f_{rep} t']}$$

where $t' = t + \frac{\varphi}{2\pi f_{rep}}$ and $f_{rep} = \frac{c}{L}$ for cavity length L. Converting this to power is as simple as squaring the equation to give:

$$P(t) = P_0 \frac{sin^2[(2n+1)\pi f_{rep} t']}{sin^2[\pi f_{rep} t']}$$

Plots of this equation versus n and t show some very important information. Figure 3 shows P vs. n for t=0 (the peak power), ϕ=0, and L=5.45 m (the length of the laser cavity in this experiment).

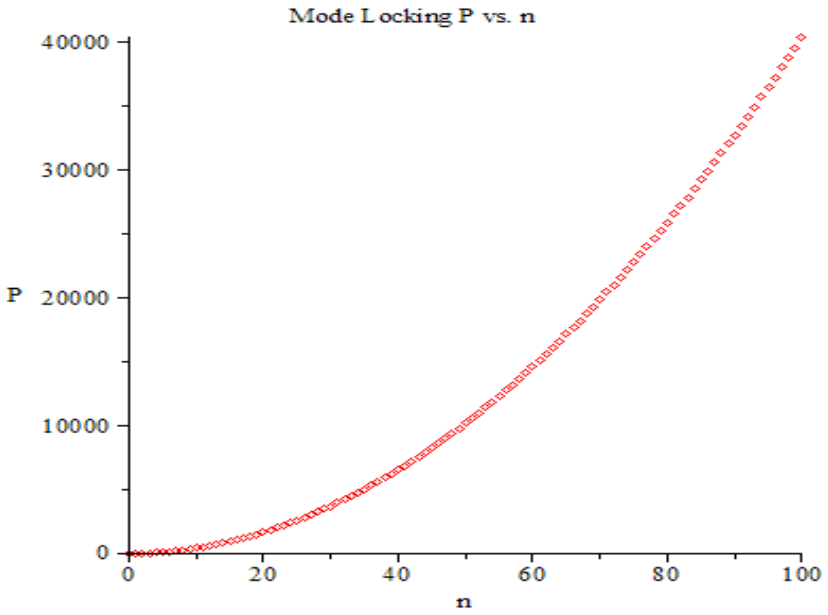

Figure 3 shows the quadratic increase in power for increasing number of cavity modes at t=0.

Notice that the peak power appears to increase quadratically for an increased number of modes in the cavity.

Next is a normalized plot of the power versus time for varied n, shown in Figure 4. Notice how the pulse width decreases with an increase in the number of modes in the cavity. This is extremely important for our purposes. Since we are looking for a pulse width ~100 fs or smaller we now know that the more modes that can be excited in the cavity, the smaller the pulse width will be.

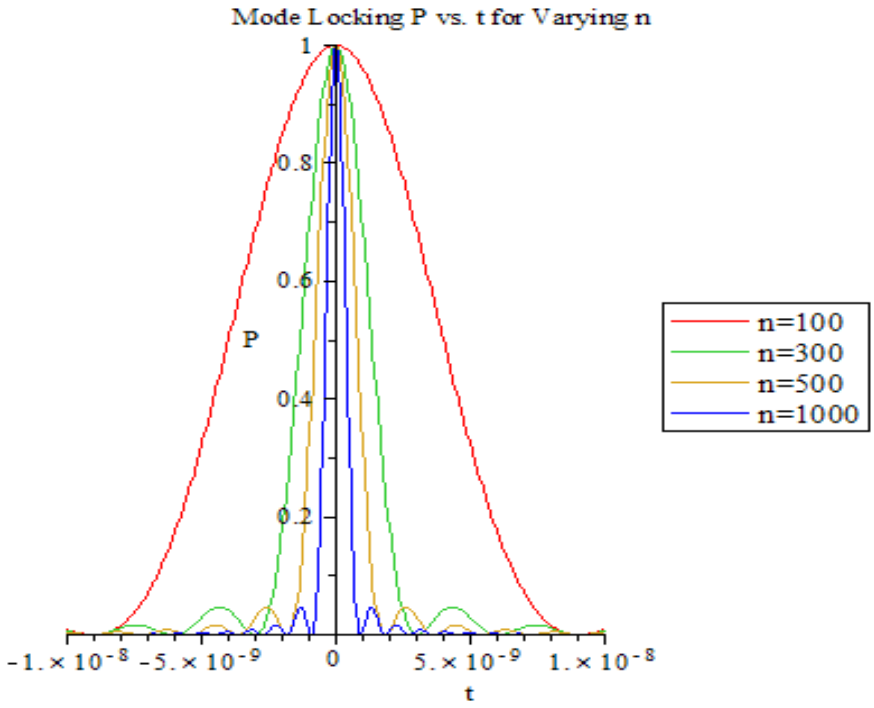

Figure 4 shows decrease in pulse widths for larger numbers of modes in the cavity.

IV. Tests

The plan for building the erbium fiber laser was to install each important part to the laser and test to see if it satisfied design specifications. The parts that were tested first were the three parts that make up any laser: the pump, the lasing medium (amplifier), and the optical cavity. The two tests after this were related to mode-locking the laser. The tests were: the pump test, the amplifier test, the enclosed laser test, the free space laser test, and the mode-locking test(s). See the" System Setup" section of the introduction for material on the function of each part within the laser.

1. Pump

The first installation and test was that of the 980 nm butterfly-mounted diode laser. The test consisted of the diode being connected to the lab's interlock system and the input current to the laser controlled. The output of the laser was connected to an optical power meter and the power measured. The current was raised in increments of 50 mA and the corresponding powers recorded. Figure 5 shows this correspondence, with power converted to dBm (see the Appendix C for information on power and dBm relationships).

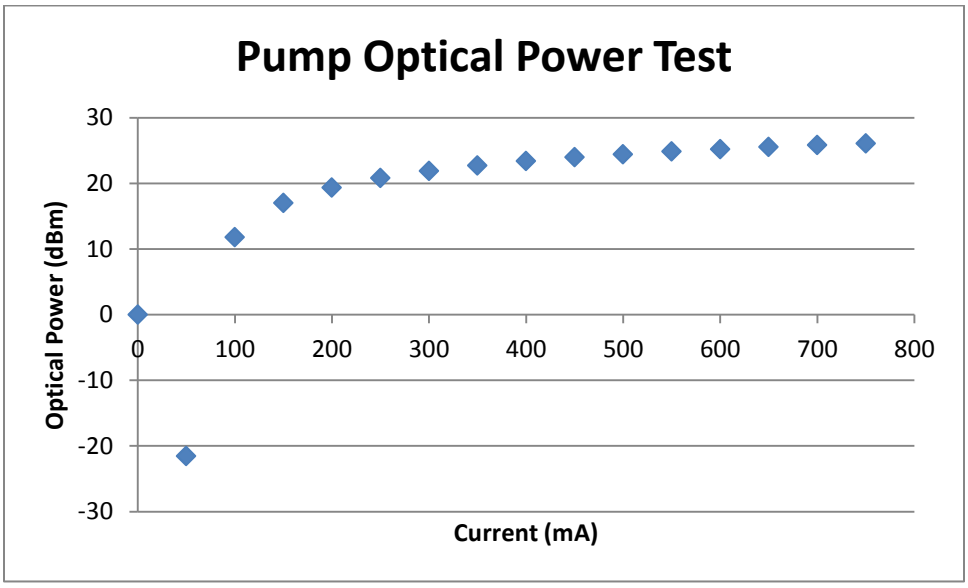

Figure 5 gives an idea of how the pump power is affected by changing current.

The purpose of this test was to have a baseline for later tests in which the amplification of the input signal comes from the pump laser.

To complete the test, the optical spectrum of the pump laser was then measured and can be seen in Figure 6.

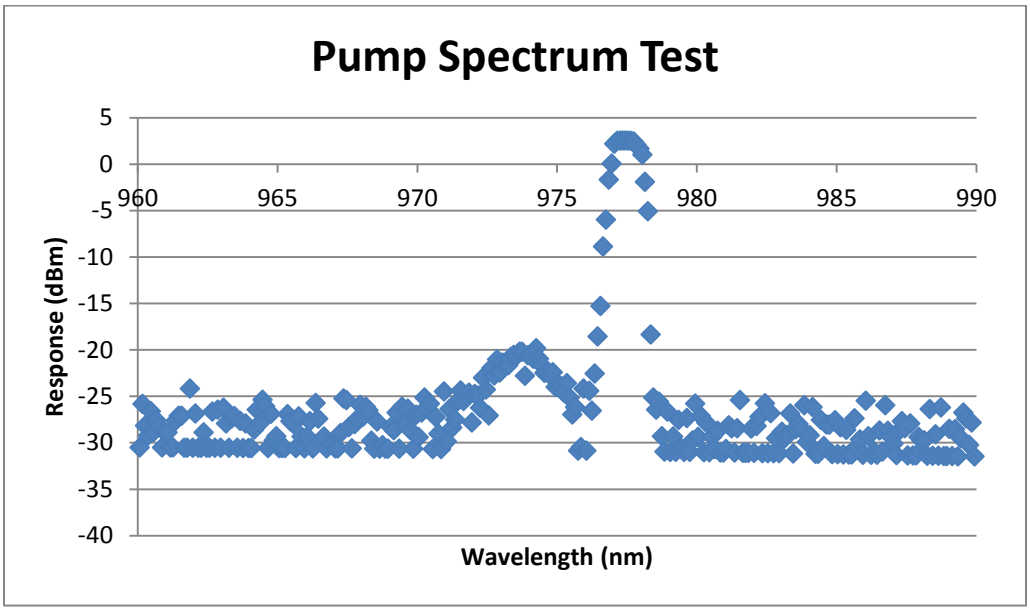

Figure 6 shows the optical spectrum of the pump, which appears to be lasing close to 980 nm.

2. Amplifier

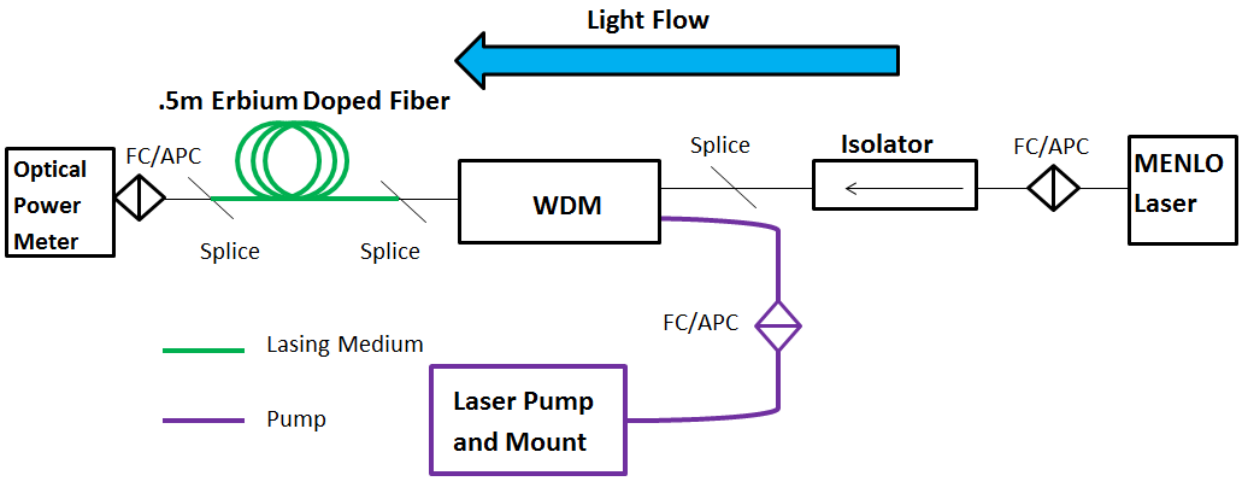

Figure 7 shows a schematic for the amplifier test.

During the amplifier test, many of the components that would later make up the laser were added (see Figure 7). From the previously-tested laser pump and mount, an FC/APC connection was made to a WDM. The other input of the WDM was spliced to the output of an isolator, the input of which was connected to an attenuated* 1550 nm MENLO laser to aid in stimulated emission of photons. The output of the WDM was spliced to the lasing medium, .5 m of erbium-doped fiber, which was connected to an optical power meter through an FC/APC connection. The current of the pump laser was increased by increments of 50mA and the power read. The data from this test was converted to dB using the input MENLO power of .0385 mW (see the Appendix C for information on power and dB relationships).

*The 10 dB attenuator that was connected to the MENLO was used to reduce the incoming power by a factor of 10 dB. The reason for this was to prevent saturation of the erbium fiber such that a more accurate reading of the amount of amplification could be attained.

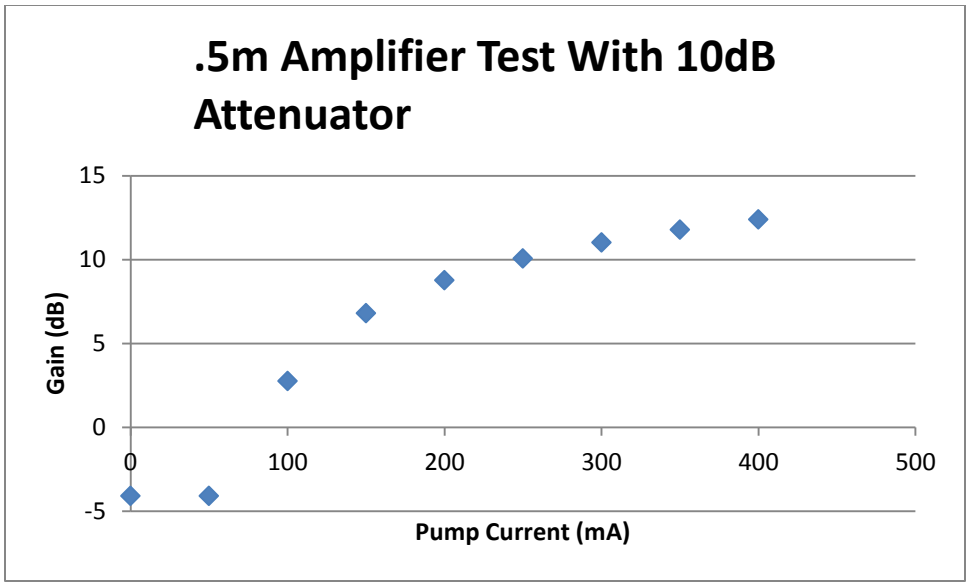

Figure 8 shows the gain vs. pump current of the amplifier, with maximum gain close to the 15 dB promised by the erbium manufacturer.

The manufacturer for the company that produced the erbium fiber stated that 15 dB of amplification for .5 m of fiber should be attainable. The data from that appears to hold true since the maximum gain value was ~15 dB, meaning that the amplifier works as intended.

3. Closed-Cavity Laser

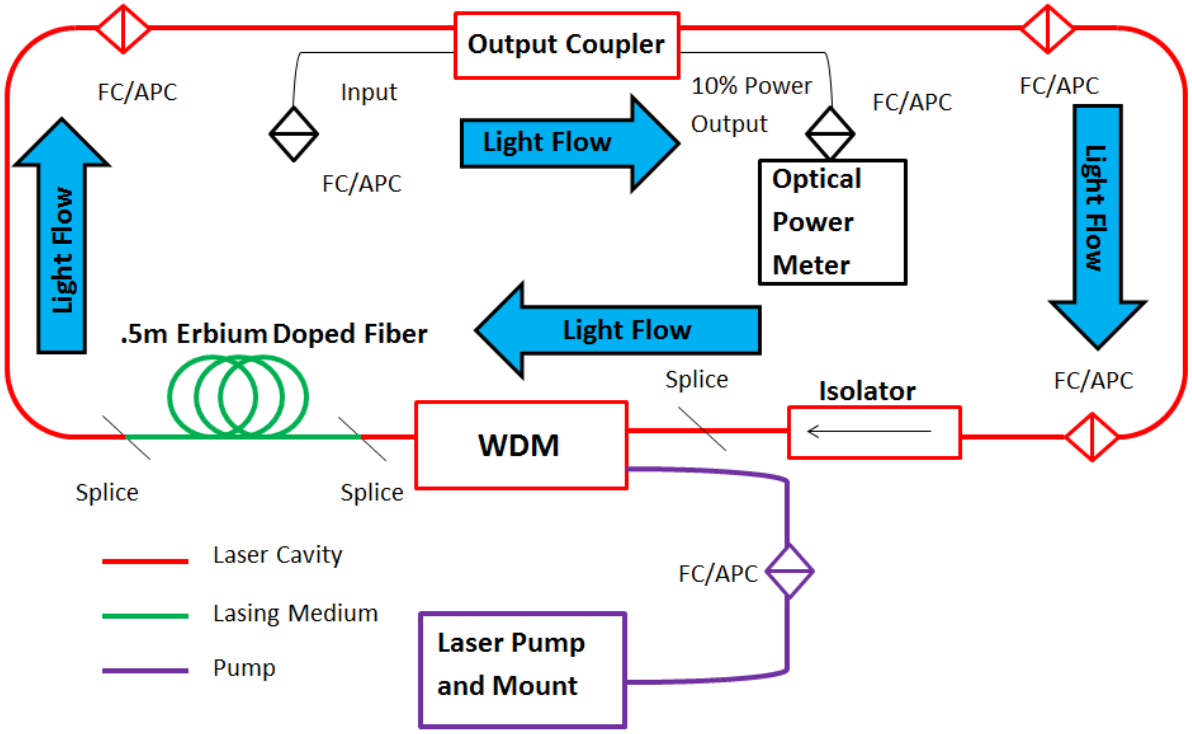

Figure 9 shows the schematic for the closed-cavity laser test.

With the success of the amplifier and pump tests, the next step in the process was to install the laser cavity and see if lasing could be achieved. The setup was very similar to the amplifier test and differs only in that the MENLO was taken out and an output coupler installed to form an enclosed laser cavity (see Figure 9). An optical power meter was connected to the 10% output lead on the output coupler and the power measured with the pump current varied. Figure 10 illustrates the results.

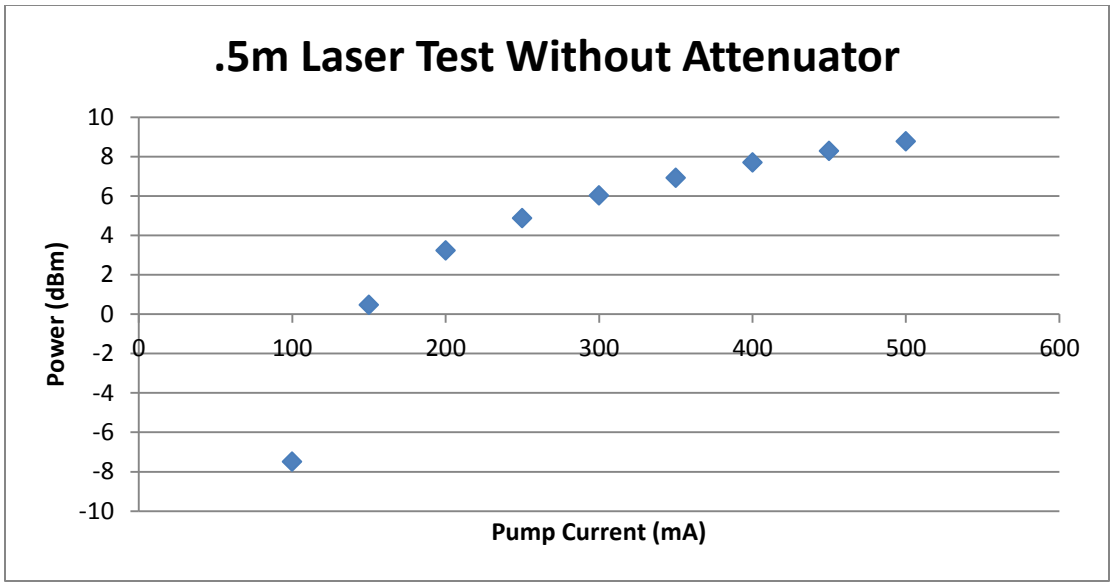

Figure 10 shows the dBm power for an input pump current andgives an idea of the laser power.

Noting the simarity of Figure 10 to Figure 8, it can be concluded that lasing was occuring in the cavity at the time of the test. To ensure that the cavity was indeed lasing as well as to see what wavelength that lasing was occuring at, the optical spectrum was taken by connecting the optical power spectrum analyzer to the output coupler instead of the powermeter. Figure 11 shows that lasing was occuring generally close to 1550 nm.

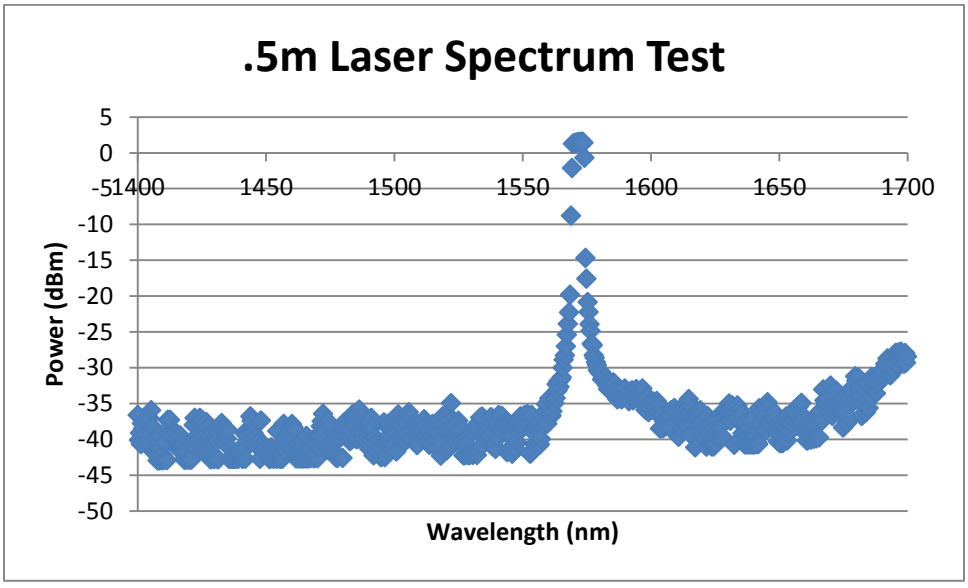

Figure 11 shows the optical spectrum of the enclosed laser and depicts lasing power at ~1550 nm.

4. Free space Laser

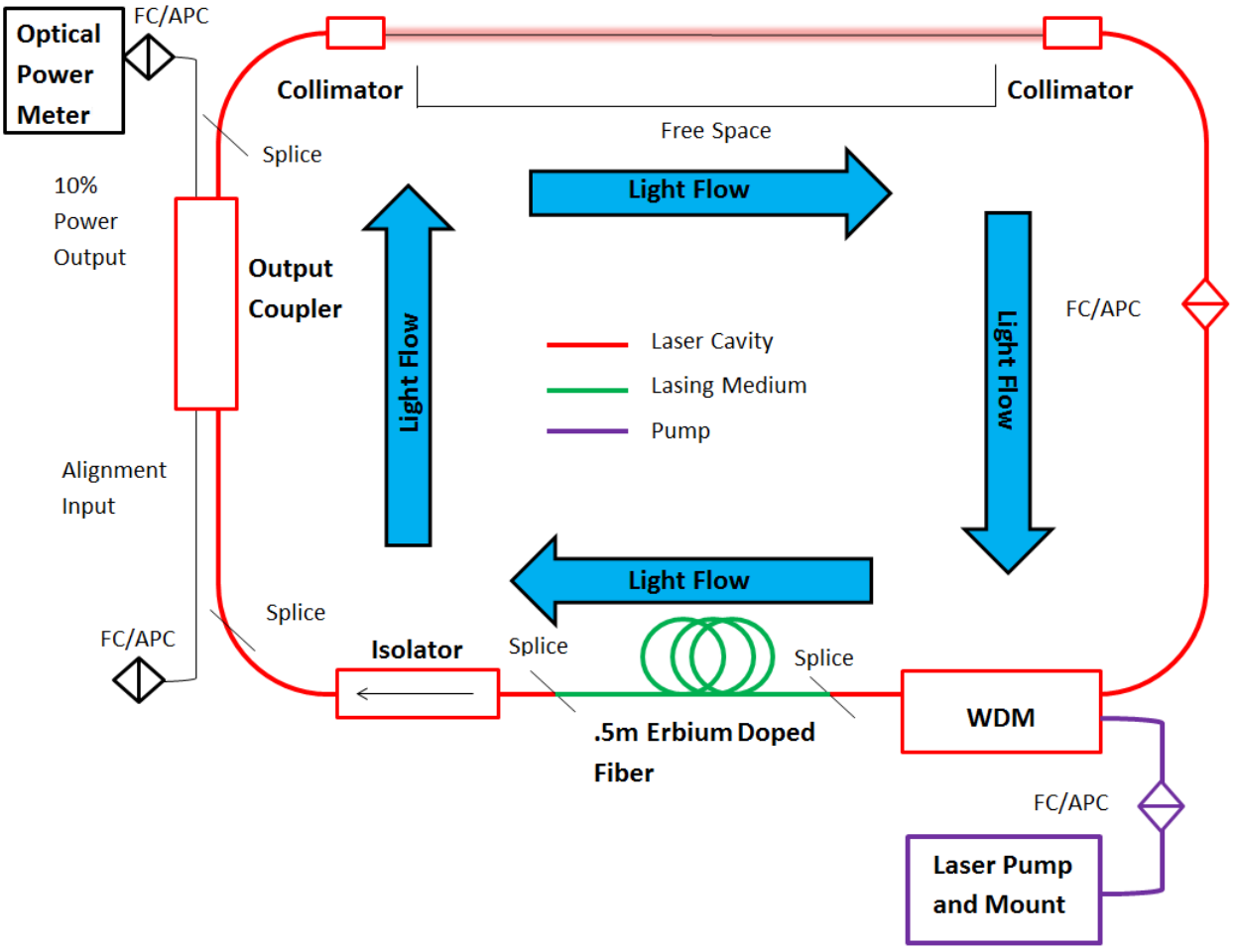

Figure 12 shows a schematic of the laser with a free space component installed.

With a working laser, the next step was to get it mode-locked, but the free space component had to first be installed with assurance that lasing still occurred. Two collimators were installed after the output coupler (see Figure 12) and aligned by connecting the MENLO to the FC/APC input of the output coupler, disconnecting the FC/APC connection between the WDM and second collimator, then connecting the optical power meter to the collimator end and adjusting the collimators such that the power reading was maximized.

After alignment, the power meter was re-connected to the 10% power output end of the output coupler, the MENLO disconnected, and the connections restored as shown in the diagram. The pump laser current was then varied and the power from the power meter recorded. Figure 13, although of a smaller density of data points than the one in the “Closed-Cavity Laser” section, is similar enough to deduce that the free space laser was still lasing.

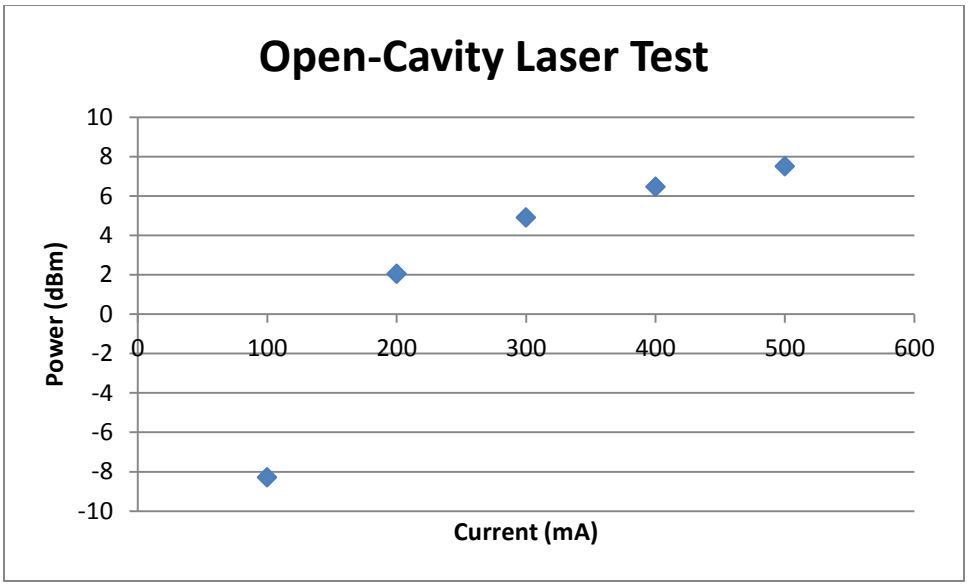

Figure 13 shows the free space laser power for an input pump current.

5. Mode-locking Laser

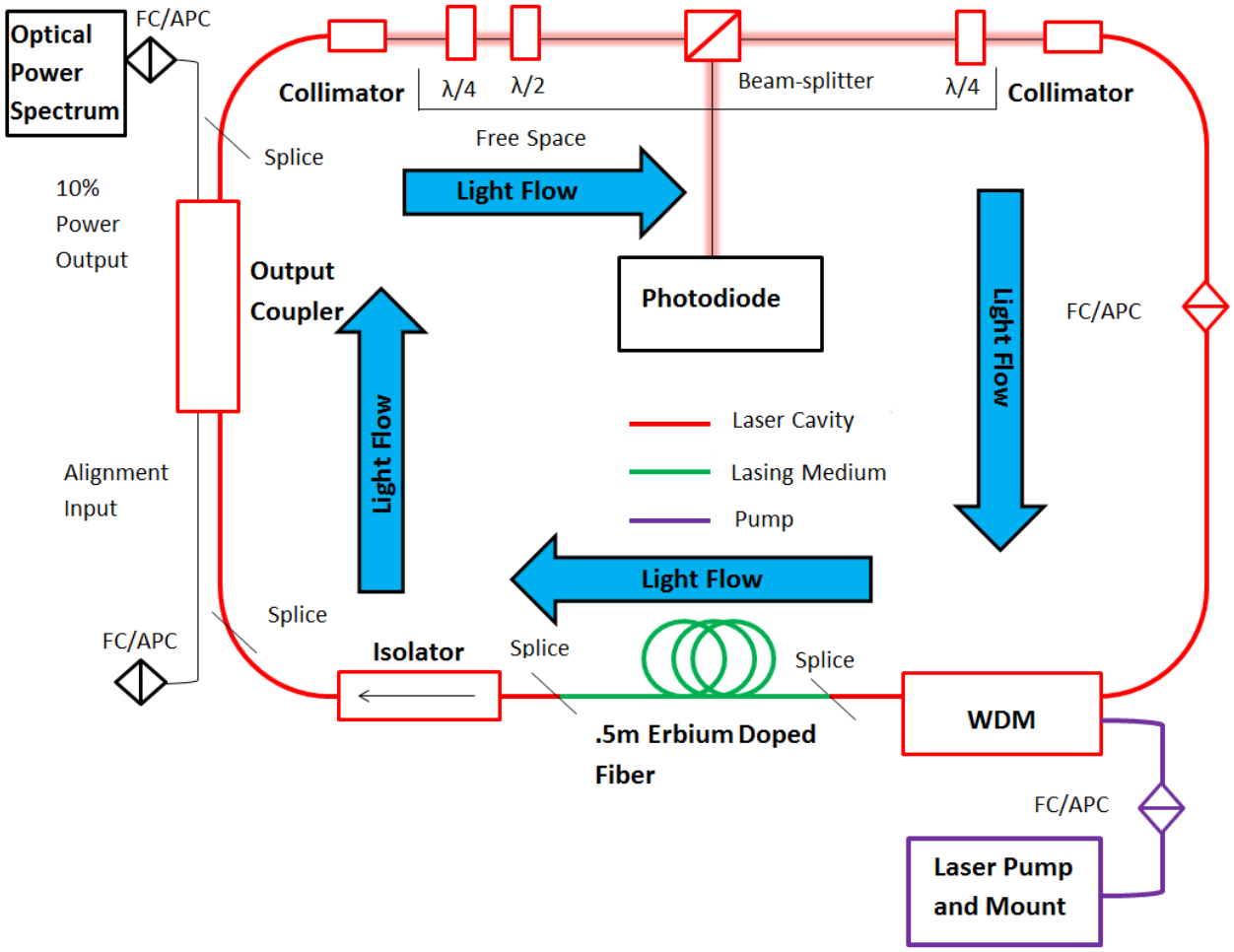

Figure 14 shows a schematic of the final mode-locked laser.

The final set of tests was to mode-lock the laser. First, the two quarter-wave plates, half-wave-plate, and beamsplitter were installed in the free space laser constructed thus far. A photodiode was aligned with one beam emitted from the beamsplitter and connected to an oscilloscope where pulses were monitored. The optical power spectrum was also monitored from the 10% output from the output coupler. The wave plates and power were each adjusted until the optical spectrum was observed to gain a large bandwidth and the oscilloscope output was observed to have large, sharp peaks. Figures 15 and 16 illustrate the results at optimized settings of*:

-Laser Current: 254 mA

-1st quarter-wave plate: 303^o

-Half-wave plate: 318^o

-2nd quarter-wave plate: 288^o

*Note: The settings given here were with random orientations of the wave plate fast axes with respect to 0^o. The results are given in order to document the optimized parameters.

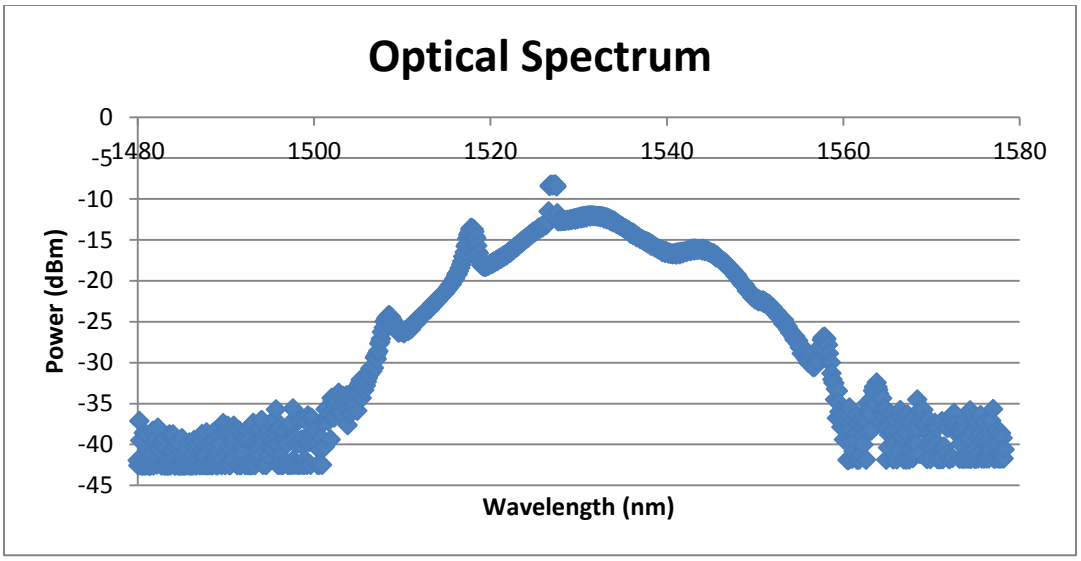

Figure 15 shows the mode-locked optical spectrum. Note broad bandwidth of wavelengths as opposed to the peak observed in Figure 11.

On the optical spectrum data, notice the broad set of wavelengths characteristic of mode-locking instead of the single peak seen in previous optical spectrums.

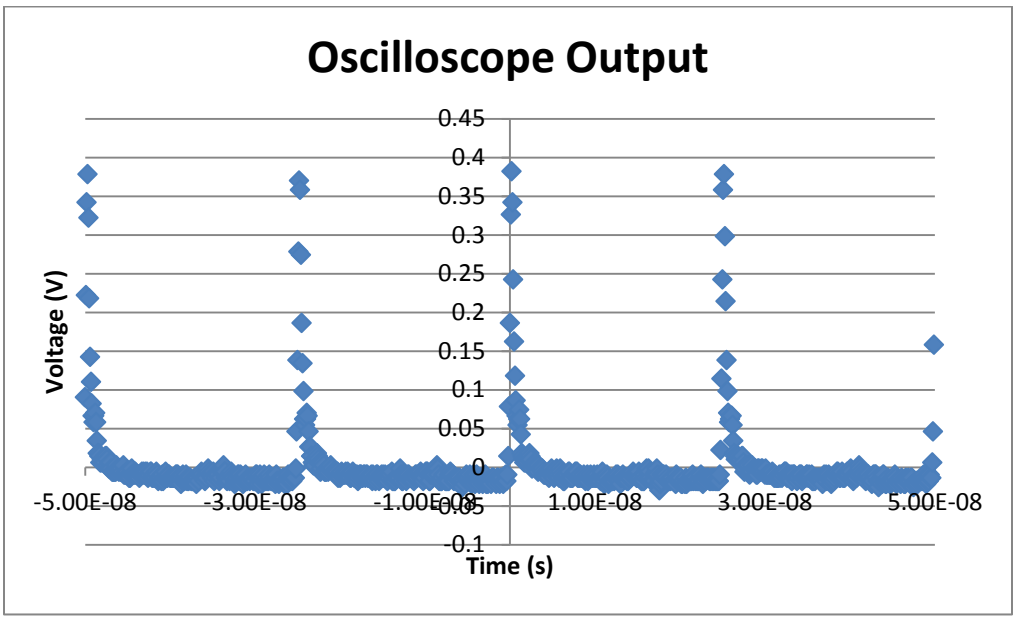

Figure 16 shows the oscilloscope output from the photodiode in the mode-locked cavity.

The oscilloscope data shows the very sharp spikes in voltage followed by little to no voltage that we would expect to see if the laser is mode-locked (see “Mode-Locking” in the theory section of the introduction for more details.).

The next thing that was tested once the laser was mode-locked was the radiofrequency spectrum (RF spectrum). This involved disconnecting the photodiode

from the oscilloscope and connecting it to another detector to see what frequency the signal was emitted at (note that the power was also measured at this time to be 2.66mW from the output coupler). Figure 17 shows the RF spectrum corresponding to the optimized oscilloscope and optical spectrum data. Notice that the peak center is at around 40 MHz. This is the frequency, which depends on the length of the cavity.

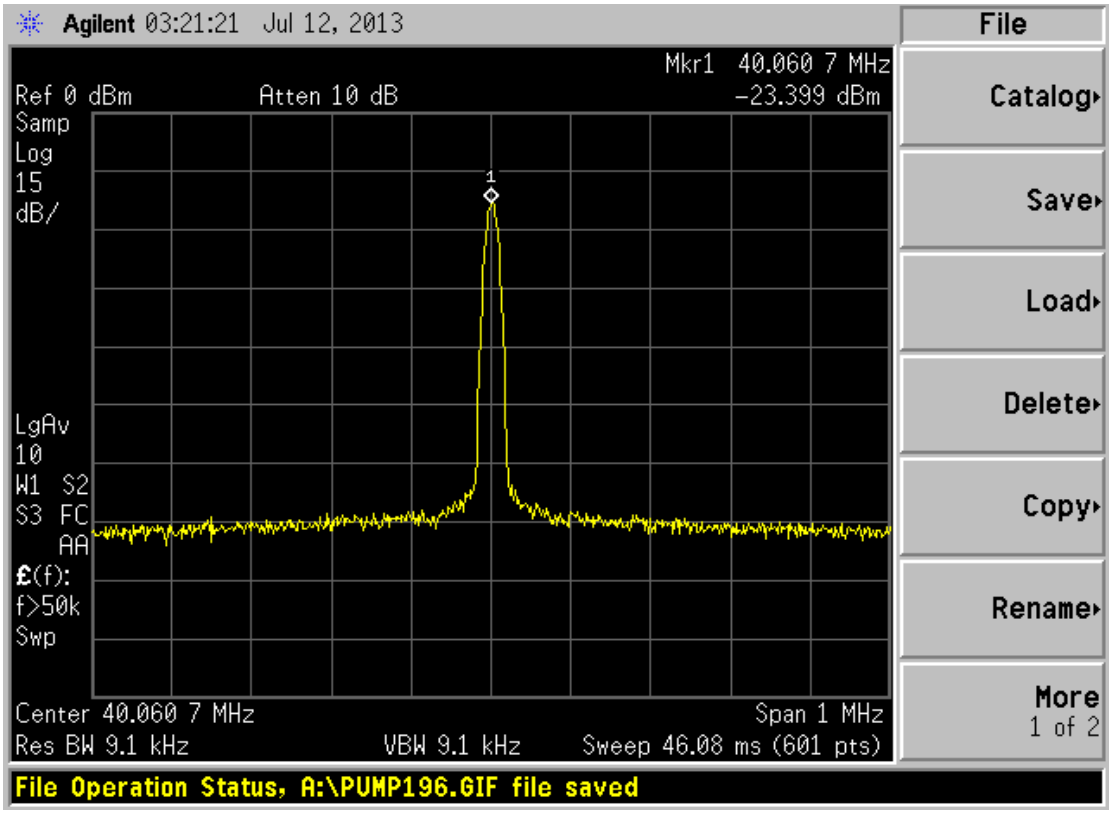

Figure 17 shows the RF spectrum of the cavity.

The final and one of the more important tests for the mode-locked laser was to find the pulse length. This involved connecting the 10% output lead from the output coupler to an autocorrelator and connecting the output from there to a detector. The details of how the pulse width was found can be seen in the Appendix D. The calculations in this section detail how a pulse width of 380.1 fs was obtained for the optimized parameters.

V. Conclusion

Many tests were performed over the course of constructing the mode-locked erbium fiber laser. The majority of the initial tests were to prove that the parts operated as desired. The pump test set to prove that the laser pump was operational as well as to gain insight into how the pump power varied with input current (Figure 5) and to find the wavelength the pump lased at shown in Figure 6 (~980 nm). The amplifier test was performed chiefly to see if 15 dB of gain could be obtained from the erbium fiber, which it was (Figure 8). The enclosed and free space laser tests proved that the laser was operational and experienced lasing at ~1550 nm (Figure 11). With optimized wave plate settings and pump current, the mode-locking tests were able to obtain a fairly broad optical spectrum (Figure 15) as well as a clean RF spectrum with no noticeable wings (Figure 17). This led to a measurement of the pulse width of 380.1 fs. This is certainly a good value to have on these initial tests. Future plans for this laser hope to obtain even smaller pulse widths by further broadening the optical spectrum using more highly-doped erbium fiber.

VI. Appendix

A) Optical Fibers 101

There are three basic parts to an optical fiber: the coating, the cladding, and the core. There are many special deviations from these parts such as dual-core fibers that do not relate to this project and therefore will not be discussed, since only the single. The coating is an outer, protective layer of the fiber that allows for delicate handling and is usually ~100μm thick. The cladding is a material with a lower refractive index than the core and also ~100μm thick. The core is usually made of glass and a few μm thick, can be doped with other material to suit experimental needs.

Optical fibers work on the principal of total internal reflection, where light in a higher index of refraction, the core in this case, incident at an angle on a material of lower refractive index, the cladding, will have 100% reflection past a certain angle of incidence. With this principle in mind, fibers are designed to trap the light inside the fiber and propagate down the length. These properties come at the price of the fiber being extraordinarily delicate and sensitive to bending. Each fiber has a certain radius of curvature past which the optical signal will depreciate significantly. Fibers also widely differ on what materials that are made of. The standard fiber is silicon based, however, the core can contain varying amounts of other elements depending on the intended purpose. Such fibers are said to be doped, such as the length of erbium fiber used in this project. Note that fibers are considered to be the standard silicon type unless explicitly stated.

B) Splicing

Splicing is the delicate and all-important task of taking two ends of optical fiber and fusing them together while minimizing the amount of power lost where the ends don't match exactly. In an ideal world, there would be absolutely no loss whatsoever from this point, however, this is never the case, so the goal becomes making the power loss negligible, usually around .01-.03 dB.

Splice work was one of the more time-consuming aspects of this project. There were several tests in which the optical signal would vanish and, much like an electrical engineer would measure voltage beginning from the source and then go stepwise through each component to find where an electrical signal vanishes, so too was a stepwise approach used to find problems. However, each time a measurement needed to be made, the fiber had to be broken and re-spliced at least once if there was not a patch cable in place that could connect to an optical power meter. One might ask, "Why not just use patch cables for each connection then?" The problem with using patch

cables is that they have a much more significant power loss associated with them than splices, usually a few dB as opposed to the very miniscule .01-.03 dB from a splice.

The standard procedure for splicing two fiber ends is to first strip off a section of the coating (usually around an inch or so) to expose the cladding using a special stripping tool, being sure to clean off any residue with a Kimwipe and cleaning solution. Next, a cleaver is used to make a very precise cut of the wire. This must be cleaned of all dust particles, as even a single speck of dust will ruin a splice. The two ends are put into a splicer which fuses them together using an electrical discharge. The splice is extremely delicate at this point, so a special sleeve is applied to cover and reinforce it.

C) Watts, dB, and dBm

For those that have not worked with the uses of the different units of power: watts, dB, and dBm, an explanation is necessary to understand the plots within this paper. Watts, or milliwatts as they were measured in for the purposes of this experiment, are simply the standard metric unit to measure power. The units of dB and dBm are simply a way to view measured powers as a ratio of the measured power to some reference power. dBm follows the equation: $P_{dBm} = 10 * \log_{10} \frac{P_{out}}{1}$, which says that the dBm power is proportional to the measured power in milliwatts versus 1 mW, and thus gives a standard scale that always references 1 mW. This is useful for showing large power ranges in a more compressed form and is used for the majority of data plots for this project. dB follows a very similar equation: $P_{dB} = 10 * \log_{10} \frac{P_{out}}{P_{in}}$, which says the dB power is proportional to the ratio of the output power versus some reference power, usually the initial input power. This is very useful for measuring the gain of a system and is always a primary concern when discussing lasers.

D) How the Autocorrelator Works

An autocorrelator is essentially a more complex version of a Michelson interferometer and is used to convert very small pulse lengths into lengths that can be measured. The actual pulse length can then be found through back-calculation from the measured pulse length. In a basic Michelson interferometer setup, laser light enters a beamsplitter and is split into two different arms. Each one has a mirror, one of them with adjustable position, that reflects the light back to the beamsplitter, and a percentage goes into a new arm with a detector. The setup for the autocorrelator essentially replaces the arm with a fixed mirror with a set of mirrors mounted on a machine-rotated arm. This arm has a set turning speed that is orders of magnitude larger than the pulse lengths input into the autocorrelator. In this way, light is reflected back into the beamsplitter only during the split second that the rotating mirror is aligned with the beamsplitter. The other big change is

that a nonlinear optical crystal in placed before the detector in order to ensure proper alignment. The following diagram gives a rough outline of the autocorrelator cavity used:

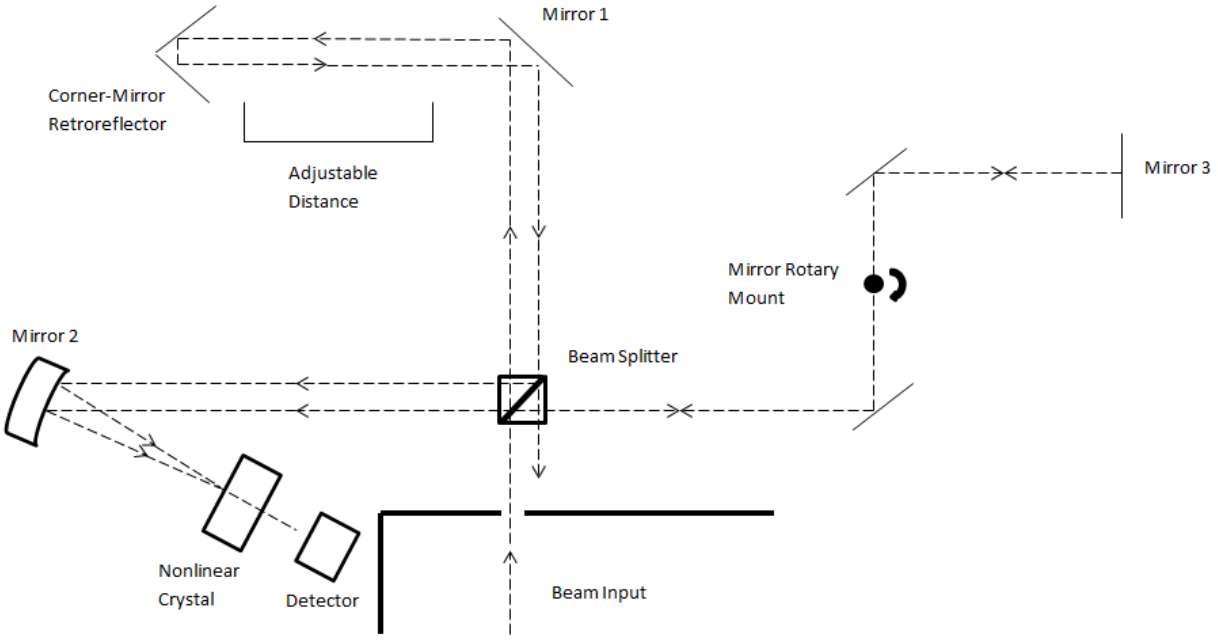

Figure 18 shows a schematic of the in autocorrelator.

The calculation to determine the actual pulse width in this experiment first required a calibration plot for the autocorrelator used. This was performed by using the 1550 nm Menlo laser as an input source of light and then measuring the change in the time scale of the peak for a certain change in the adjustable arm position of the autocorrelator. The following plot shows the results of this measurement with the distance converted into the time it takes for the light to travel within the autocorrelator using: $\frac{1}{v} = \frac{1}{c} = \frac{1}{3*10^{14}} = 3.33 * 10^{-15} \frac{s}{\mu m} = 3.33 \frac{fs}{\mu m}$. Using this and the fact that the change in travel distance is twice the change in cavity length, the time in fs was obtained:

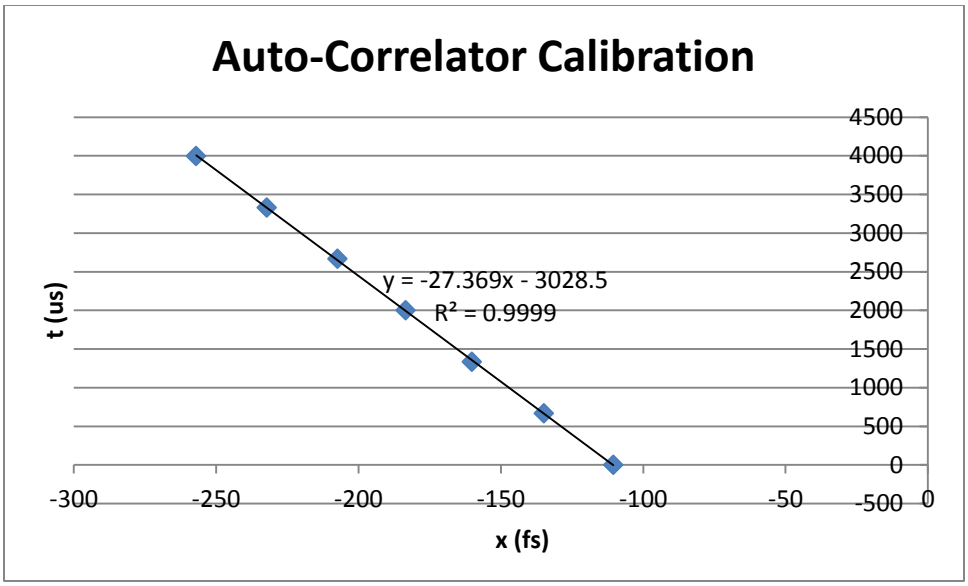

Figure 19 shows a calibration of the autocorrelator used to determine the pulse width.

The slope obtained here of 27.369 $\frac{fs}{\mu s}$ gives a conversion factor to convert the time in the measured autocorrelator full-width half-maximum into the actual input pule length after an additional multiplication by 0.7*.

After the calibration was performed, the signal from the erbium fiber laser was input into the autocorrelator. The following plot shows this signal:

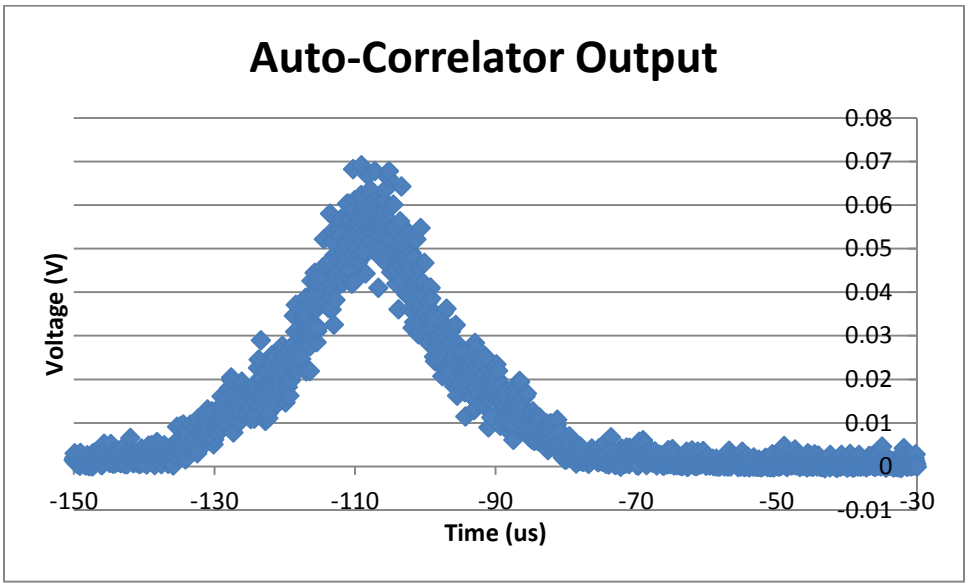

Figure 20 shows the output signal from the autocorrelator, the full-width half-maximum of which is used to determine the input signal's pulse width.

The measured full-width half-maximum from this plot gives a pulse length of -19.839, so by performing the calculation: $Pulse\ Length = (FWHM) * (Slope) * (.7) = (-19.839) * (-27.369) * (.7) = 380.1\ fs$.

*Note: The 0.7 term in the conversion is due to design specifications of the autocorrelator used and simply has to do with how the autocorrelator interacts with the input signal.

VII. References

1. Winter, Axel. *Fiber Laser Master Oscillators for Optical Synchronization Systems*. Diss. Zugl.: Hamburg, Univ., Diss., 2008, 2008. N.p.: n.p., n.d. Print.